

Impedance-matched low-pass stripline filters

D. F. Santavicca and D. E. Prober

Department of Applied Physics, Yale University, New Haven, Connecticut 06520-8284

(10 February 2008)

We have constructed several impedance-matched low-pass filters using a stripline geometry with a dissipative dielectric. The filters are compact, simple to construct, and operate in cryogenic environments. The dissipative dielectric consists of magnetically-loaded silicone, which is commercially available in several varieties under the trade name Eccosorb. For a stripline length of 32 mm, the filters have a passband that extends from dc to a 3 dB bandwidth between 0.3 and 0.8 GHz. The 3 dB bandwidth can be adjusted beyond this range by changing the length. An extremely broad stopband at higher frequencies, with attenuation exceeding 100 dB, is achieved along with a return loss greater than 10 dB measured up to 40 GHz. This combination of high attenuation and low reflected power across a broad stopband ensures that spurious or unwanted signals outside the passband do not reach or return to the device. This type of filter has applications in microwave frequency measurements of sensitive non-linear devices such as heterodyne mixers, quantum tunneling devices, and quantum computing elements.

84.40.Az, 84.20.Vn, 84.32.-y, 77.22.Gm

Introduction

An impedance-matched low-pass filter simultaneously maintains high attenuation and low reflection across a very broad high-frequency stopband. This ensures an impedance close to 50Ω over many decades in frequency. Specifications for most microwave devices assume that all ports are properly terminated at all relevant frequencies. In strongly non-linear quantum devices, the termination impedance can have a significant effect on the device performance. Termination by an incorrect impedance can have a detrimental effect which may be difficult to model or predict. Conventional reactive filters deviate significantly from 50Ω outside their passband, as do most amplifiers

outside of their amplification band. An impedance-matched low-pass filter can be used to ensure that a port remains properly terminated even at very high frequency.

One application of such a filter is in the microwave characterization of heterodyne mixers, including superconducting tunnel junction and bolometric mixers. As a non-linear device, the heterodyne mixer responds at multiple frequencies in addition to the input frequencies. To avoid spurious effects, the local oscillator power reflected by the mixer and also the higher harmonics generated and emitted by the mixer need to be properly terminated at the intermediate frequency port. The impedance-matched low-pass filter ensures a low level of reflected power out to very high frequency while efficiently transmitting the intermediate frequency output, which is in the filter's passband. Another potential application is filtering the lines used to manipulate quantum bits with fast pulse sequences, as well as the high-frequency readout lines, provided that the filter bandwidth is sufficiently large.

One method of achieving an extremely broad stopband is to have spatially distributed circuit elements instead of lumped-element components. Lumped elements typically have a stopband that is limited by parasitics. Several types of non-impedance-matched distributed filters have been reported, primarily for filtering the biasing lines of single-electron and quantum computing circuits. The most widely used is the metal powder filter, which consists of a wire embedded in a mixture of metal powder and epoxy.^{1,2,3} This low-pass filter utilizes the large capacitance between the wire and the powder as well as eddy-current dissipation in the powder. Microfabricated versions of such non-impedance-matched distributed filters have also been reported.^{4,5} The passband can be as low as MHz, or larger.

To achieve impedance matching, a distributed filter must be constructed in a transmission line geometry with frequency-dependent dissipation in the conductor or the dielectric. Previous work described a filter based on the resistive coaxial cable Thermocoax.⁶ An attenuation of approximately 100 dB at 10 GHz is achieved with a cable length of 6 cm. The 3 dB bandwidth for a cable of this length is ~ 1 GHz and the return loss in the

stopband is approximately 6 dB.⁷ An impedance-matched version of the metal powder filter, constructed in a coaxial geometry, has recently been reported.⁸ This filter displays a 3 dB bandwidth of approximately 0.3 GHz with a length of approximately 6 inches. At 10 GHz, it displays up to 90 dB of attenuation with a return loss of 35 dB. Reflection data was only reported for this single frequency.

We describe a filter that uses a magnetically-loaded dielectric in a stripline geometry. This filter exploits a combination of magnetic and dielectric dissipation to achieve a stopband attenuation that exceeds 100 dB. The filter also demonstrates a return loss greater than 10 dB out to 40 GHz. At high frequency, this represents significantly greater attenuation per unit length than the coaxial metal powder filter and better impedance matching than the Thermocoax filter.

Filter Design

A stripline geometry was chosen because it is easier to construct than a coaxial geometry but, unlike a microstrip, the field lines are entirely inside the dielectric, maximizing the dissipation. The stripline supports a TEM mode at low frequency, with higher order modes appearing when the enclosure begins to act as a waveguide.⁹

To determine the attenuation constant, we consider a TEM mode in a transmission line with a complex permittivity and permeability.¹⁰ The permittivity can be expressed as $\epsilon = \epsilon' - j\epsilon'' = |\epsilon|e^{j\delta_\epsilon}$ where $\tan \delta_\epsilon = \epsilon''/\epsilon'$ is the dielectric loss tangent. Similarly, the permeability can be expressed as $\mu = \mu' - j\mu'' = |\mu|e^{j\delta_\mu}$ where $\tan \delta_\mu = \mu''/\mu'$ is the magnetic loss tangent. The complex propagation constant is $\gamma = \alpha + j\beta = j\omega\sqrt{\epsilon\mu}$, where α is the attenuation constant, β is the phase constant, and ω is the angular frequency. For propagation in the x direction, the electric field magnitude is $E(x) = E(0)e^{i\gamma x}$. We can

express $\alpha = \text{Re}[\gamma] = \omega\sqrt{|\epsilon||\mu|} \sin\left(\frac{\delta_\epsilon + \delta_\mu}{2}\right)$, which can be written using the above

relations as

$$\alpha = (1.48 \times 10^{-8}) f \sqrt{\frac{\mu' \varepsilon'}{\mu_0 \varepsilon_0}} \left\{ \sqrt{\left[1 + \left(\frac{\varepsilon''}{\varepsilon'} \right)^2 \right] \left[1 + \left(\frac{\mu''}{\mu'} \right)^2 \right]} - 1 + \left(\frac{\varepsilon''}{\varepsilon'} \right) \left(\frac{\mu''}{\mu'} \right) \right\}^{1/2} \quad (1)$$

in units of Np/m, where f is the frequency and μ_0 and ε_0 are the free space permeability and permittivity, respectively. The transmitted power is thus $P_{trans} = P_{inc} e^{-2\alpha L}$, where L is the length of the stripline in the dielectric. The attenuation scales with the length but is otherwise independent of the transmission line geometry and is only a function of the dielectric material. Magnetically-loaded dielectrics provide very high attenuation because they typically have a magnetic loss tangent that increases with frequency combined with a large permittivity.

The overall filter dimensions are 57 x 19 x 17 mm. A rectangular cavity, machined in a block of copper, defines the outer dimensions of the stripline. The cavity has a depth of either 2.0 mm or 1.5 mm and lateral dimensions of 32 mm x 13 mm (length x width). On the bottom of the cavity, as well as on the top Cu piece that covers the cavity, a sheet of adhesive-backed Eccosorb material is cut to size and attached. The Eccosorb thickness is either 1.0 mm or 0.76 mm and fills the cavity when the top and bottom pieces are attached.

Eccosorb is a family of microwave absorbing materials produced by Emerson & Cuming.¹¹ It is commonly used to attenuate microwave reflections from surfaces or to reduce unwanted cavity resonances inside metallic enclosures. It comes in carbon- and magnetically-loaded varieties in different thicknesses and with several dielectric embedding materials. We use the 1.0 mm thick MCS and FGM-40 materials, as well as the 0.76 mm thick GDS material, all of which are magnetically-loaded silicones. The magnetic loading material is carbonyl iron or ferrite powder, or a combination of the two.

Two SMA receptacles with an extended dielectric and pin contact¹² are mounted on each end of the bottom Cu piece such that the pins extend into the center of the cavity from each end. Connecting the pins is a strip cut from a sheet of 0.15 mm thick Cu foil. The

ends of the strip are soldered to each pin contact. An image of two completed filters is presented in figure 1.

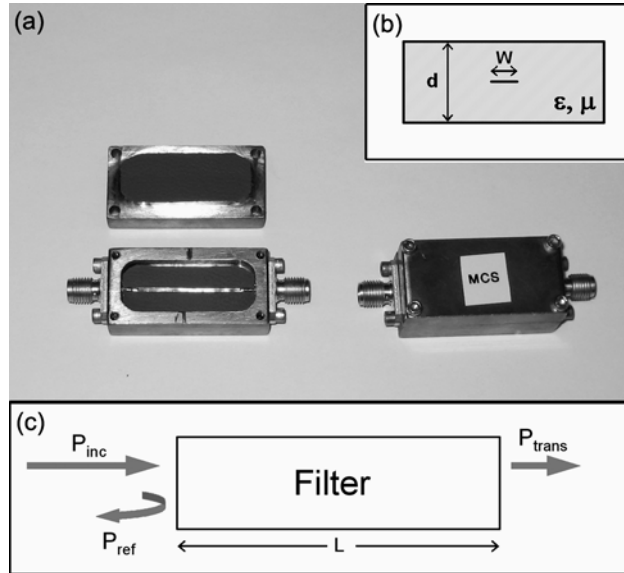


FIG. 1. (a) Photograph of two completed filters, one open and one closed. (b) Sketch of the stripline geometry, shown in a cross-sectional cut viewed from the end. The width of the cavity is $\gg W, d$. (c) Filter block diagram.

The center conductor width W was chosen by testing strips of different widths and selecting the one that gave the lowest average return loss in the measurement range 50 MHz – 40 GHz. We chose $W = 1.1$ mm for the MCS and FGM-40 materials and $W = 0.8$ mm for the thinner GDS material. Introducing a slight taper on each end of the center conductor further improved the reflection coefficient by creating a gradual transition from the pin to the wider center conductor. The stripline geometry assumes that the side walls do not significantly alter the field lines. This condition is valid if the width of the stripline cavity is much greater than the width of the center conductor. In our design, the cavity width is more than ten times the width of the center conductor.

Filter Characterization

The attenuation and return loss of the stripline filters made from the three different Eccosorb materials were measured at room temperature, 77 K, and 4.2 K using an HP 8722D 50 MHz – 40 GHz network analyzer. For testing at 77 K and 4.2 K, the filter was

immersed in liquid nitrogen and liquid helium, respectively. The filter performance was unchanged after multiple thermal cycles. (To ensure that the silicone Eccosorb material is not degraded by thermal cycling, a sample of the MCS material was cycled between 77 K and room temperature 75 times. No signs of physical degradation, such as brittleness or cracking, were observed.) The attenuation of each filter is presented in figure 2. The 3 dB bandwidth increases as the temperature is lowered for all three filters. This is likely due to a decrease in the permittivity with decreasing temperature.

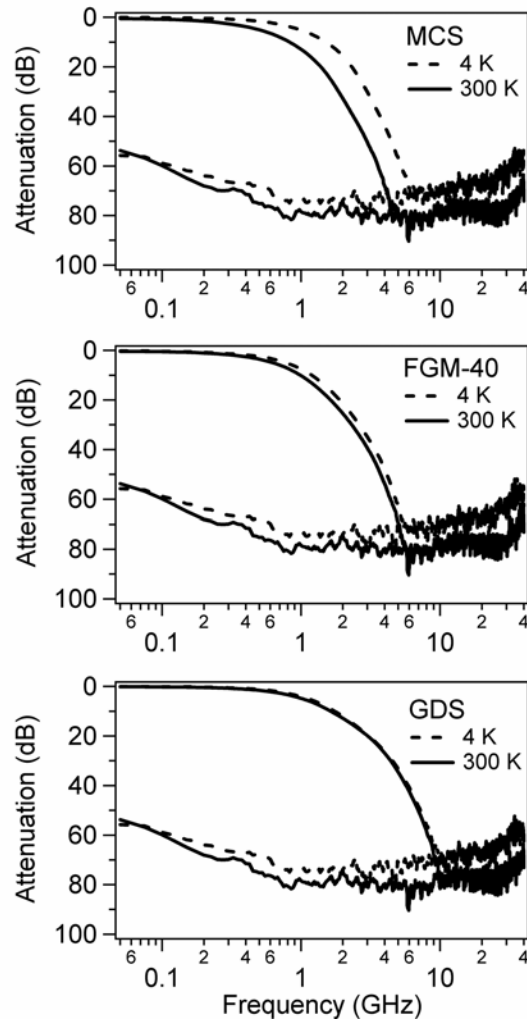


FIG. 2. Measured attenuation of the MCS, FGM-40, and GDS stripline filters at room temperature (solid line) and 4.2 K (dashed line). The instrument noise floor is indicated in grey. (The noise floor is higher at 4.2 K because of the loss of the extra cables used to measure at low temperature.)

The signal can no longer be seen above the instrument noise floor above ~10 GHz. Separate measurements were carried out using an Agilent E8254A signal generator and an HP8593E spectrum analyzer. Using a 1 kHz resolution bandwidth, the noise floor of the spectrum analyzer at 10 GHz was approximately -100 dBm. Using a source power of 0 dBm, we could determine the frequency above which the filter displays greater than 100 dB of attenuation ($f_{100\text{dB}}$). These results, along with the 3 dB bandwidths ($f_{3\text{dB}}$), are summarized in table 1.

TABLE 1. Summary of filter bandwidths at different temperatures.

	$f_{3\text{dB}}$	$f_{3\text{dB}}$	$f_{3\text{dB}}$	$f_{100\text{dB}}$
Dielectric Material	(GHz), 4.2 K	(GHz), 77 K	(GHz), 295 K	(GHz), 295 K
MCS	0.72	0.41	0.34	5.6
FGM-40	0.58	0.54	0.45	6.6
GDS	0.83	0.79	0.75	12.1

Modifying the length of the stripline will modify the attenuation, enabling the bandwidth to be optimized for a particular application. We use the length dependence of the attenuation from equation 1 to calculate the 3 dB bandwidth as a function of stripline length given the measured attenuation for a length of 32 mm. The results are presented in figure 3 for all three filters at room temperature and 4.2 K. Given the inherent tradeoff between bandwidth and stopband attenuation, we note that filters with bandwidths greater than 1 GHz may no longer have sufficient attenuation for some applications.

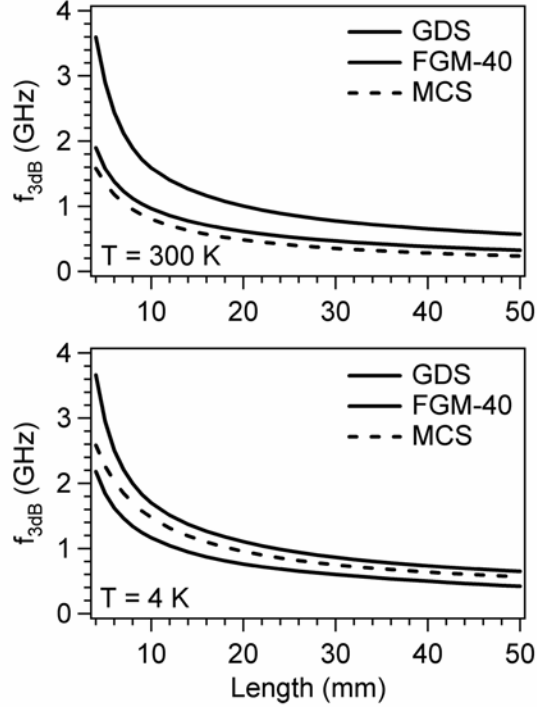


FIG. 3. Calculated 3 dB bandwidth for filters of different stripline lengths at both room temperature (top) and 4.2 K (bottom).

For comparison of different filter designs, we plot in figure 4 the attenuation of the MCS stripline filter along with a microstrip filter made from the same MCS material, a non-impedance-matched metal powder filter, and a commercial low-pass filter. The microstrip consists of a thin metal strip on top of a dielectric layer and a ground plane, with free space above the strip. The microstrip filter is the same length as the stripline filter and has a strip width of 2.5 mm and a dielectric thickness of 1.0 mm. The metal powder filter was made from a coil of Cu wire embedded in a mixture of -325 mesh Cu powder and Stycast 1266 epoxy. At room temperature, the dc resistance of the powder filter is 6.2Ω and the capacitance to ground is 1.9 nF. The commercial filter is a Mini-Circuits SLP-600,¹³ a 600 MHz low-pass filter made from reactive lumped-element components. The impedance-matched filter we developed has dramatically better stopband performance than the commercial filter. The commercial filter, however, displays a much sharper roll-off. To achieve both a sharp roll-off and a broad stopband, the impedance-matched stripline filter can be used in series with a commercial filter (the SLP filter is also cryo-

compatible), although this combination will not be impedance-matched over the entire frequency range.

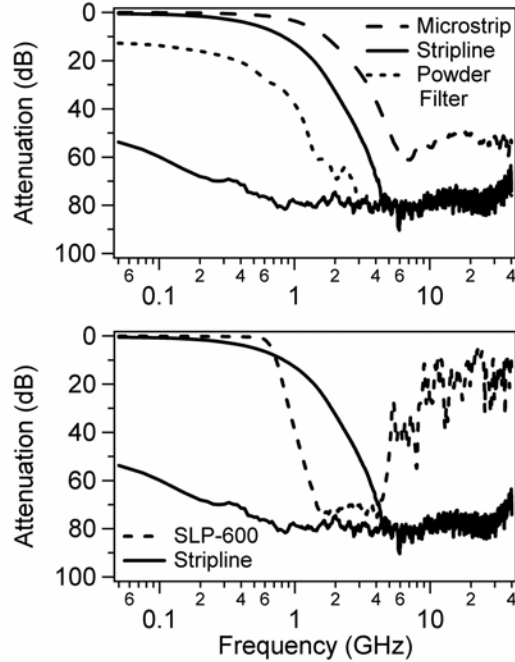


FIG. 4. Comparison of the attenuation of the MCS microstrip and stripline filters, and a metal powder filter (top). Comparison of the MCS stripline filter and a Mini-Circuits SLP-600 low-pass filter (bottom). All data are at room temperature, and the instrument noise floor is indicated in grey.

The return loss is approximately the same for all three filters and is dominated by the coaxial-to-stripline transition. The return loss of the GDS stripline filter, which is representative of all three filters, is plotted in figure 5. At all temperatures, the filter displays a return loss greater than 10 dB out to 40 GHz. The return loss is slightly lower at low temperature than at room temperature, which is likely related to a temperature-dependent permittivity. (The width of the center conductor was optimized at room temperature.) For comparison, we also plot the return loss of the metal powder filter and the SLP-600 commercial low-pass filter.

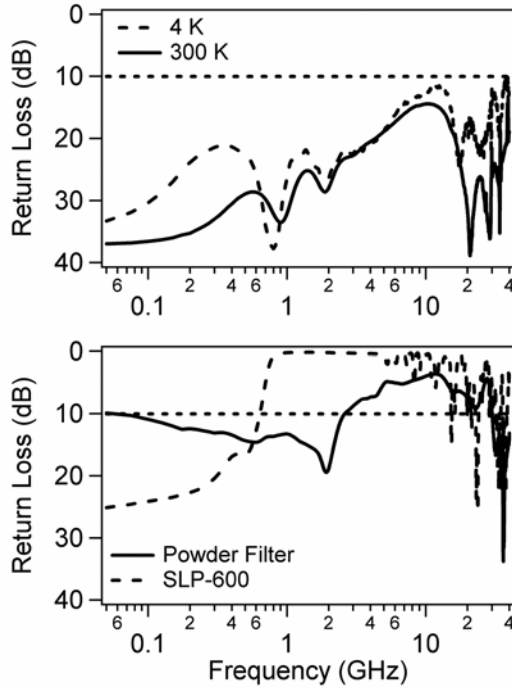


FIG. 5. Return loss of the GDS stripline filter at room temperature and 4.2 K (top). Return loss of the metal powder filter and the Mini-Circuits SLP-600 filter at room temperature (bottom). For reference, 10 dB (10% reflected power) is indicated on both plots by the dashed grey line.

For the stripline filters, a sufficiently large external field will saturate the internal magnetization, decreasing the permeability and hence the attenuation. At room temperature, the 3 dB bandwidth of the MCS stripline filter increased from 0.34 to 0.65 GHz with an external field of approximately 0.1 T applied perpendicular to both the direction of signal propagation and the flat side of the center conductor. The filter bandwidth returned to its original zero-field value upon removal of the external field.

Performance of the filters at sub-Kelvin temperatures has not yet been tested. One potential issue is thermalization. As the filter is strongly absorbing in its stopband, it will also have be an efficient emitter of thermal (blackbody) noise, with a total noise power given by the one dimensional Planck spectrum.¹⁴ In the Rayleigh-Jeans limit, this simplifies to the Johnson noise result, with a noise power per unit bandwidth of $k_B T$, where T is the physical temperature of the filter dielectric material. For measurements of ultra-sensitive devices, having the filter at low temperature is important for minimizing

the noise power seen by the device. We note that the silicone Eccosorb material used in our filters is not expected to be as easily heat sunk as the loaded epoxy of the metal powder filter. To test this, one would need a sample whose demonstrated performance depended strongly on the noise of the electromagnetic environment. Eccosorb is also available in a castable epoxy, which may be preferable to the silicone material in applications where low temperature thermalization is critical. The magnetic permeability and lossiness may be an additional consideration at temperatures below 0.1 K.

Acknowledgement

This work was supported by NSF-CHE, NSF-DMR and Yale University. We thank M. H. Devoret, V. Manucharyan and F. P. Milliken for helpful discussions.

-
- ¹ J. M. Martinis, M. H. Devoret, and J. Clarke, *Phys. Rev. B* **35**, 4682 (1987).
- ² A. Fukushima, A. Sato, A. Iwasa, Y. Nakamura, T. Komatsuzaki, and Y. Sakamoto, *IEEE Trans. Instrum. Meas.* **46**, 289 (1997).
- ³ K. Bladh, D. Gunnarsson, E. Hurfeld, S. Devi, C. Kristoffersson, B. Smalander, S. Pehrson, T. Claeson, P. Delsing, and M. Taslakov, *Rev. Sci. Instrum.* **74**, 1323 (2003).
- ⁴ D. Vion, P. F. Orfila, P. Joyez, D. Esteve, and M. H. Devoret, *J. Appl. Phys.* **77**, 2519 (1995).
- ⁵ I. Jin, A. Amar, and F. C. Wellstood, *Appl. Phys. Lett.* **70**, 2186 (1997).
- ⁶ A. B. Zorin, *Rev. Sci. Instrum.* **66**, 4296 (1995).
- ⁷ The attenuation is defined as $-10 \log (P_{\text{trans}}/P_{\text{inc}})$, with the powers defined as in figure 1(c). An attenuation of 100 dB corresponds to a power ratio of 10^{-10} . The 3 dB bandwidth is the frequency at which the attenuation is 3 dB, or approximately 1/2 in linear units. The return loss is defined as $-10 \log (P_{\text{ref}}/P_{\text{inc}})$.
- ⁸ F. P. Milliken, J. R. Rozen, G. A. Keefe, and R. H. Koch, *Rev. Sci. Instrum.* **78**, 024701 (2007).
- ⁹ D. M. Pozar, *Microwave Engineering*, 3rd edition (John Wiley & Sons, Hoboken, NJ, 2005).
- ¹⁰ P. Schiffres, *IEEE Trans. Electromag. Compat.* **6**, 55 (1964).
- ¹¹ Emerson and Cuming Microwave Products (Randolph, MA).
- ¹² Applied Engineering Products (New Haven, CT), part #9308-1113-001.
- ¹³ Mini-Circuits (Brooklyn, NY).
- ¹⁴ A. R. Kerr, *IEEE Trans. Microwave Theory Tech.* **47**, 325 (1999).